

## FEDSM-ICNMM2010-30603

### AN ANALYSIS OF SATURATED CRITICAL HEAT FLUX IN MICRO/MINI-CHANNELS

Zan Wu, Wei Li\*, Zhike Wang

Zhejiang University, Department of Energy Engineering, Hangzhou, Zhejiang 310027, China

\*Corresponding author, Tel: 86-571-87952244; Fax: 86-571-87952244; E-mail: [weili96@zju.edu.cn](mailto:weili96@zju.edu.cn)

#### ABSTRACT

This paper verified the macro-to-micro-scale transitional criterion  $BoRe_1^{0.5} = 200$  proposed by Li and Wu [W. Li, Z. Wu, A general criterion for evaporative heat transfer in micro/minichannels, International Journal of Heat and Mass Transfer 53 (2010) 1967-1976] because data points where  $BoRe_1^{0.5} \leq 200$  and  $BoRe_1^{0.5} > 200$  show very different trends for the entire database (1,672 data points). For the 859 data points with  $BoRe_1^{0.5} \leq 200$ , the boiling number at CHF decreases greatly with length-to-diameter ratio  $L_h/d_{he}$  when  $L_h/d_{he}$  is small, while  $L_h/d_{he}$  presents negligible effect on the boiling number when  $L_h/d_{he} > 150$ . For the region where  $L_h/d_{he} \leq 150$  and  $BoRe_1^{0.5} \leq 200$ , a simple saturated CHF correlation was proposed by using the boiling number, length-to-diameter ratio, and exit quality. Heated length and heated equivalent diameter were adopted in the length-to-diameter ratio, considering the actual heat transfer conditions. A combined dimensionless number  $We_m Ca_l^{0.8}$  was introduced to correlate the micro/mini-channel database for the region:  $L_h/d_{he} > 150$  and  $BoRe_1^{0.5} \leq 200$ . The new method can predict the overall micro/mini-channel database accurately on the whole. It can predict almost 95.5% of the non-aqueous data and 93.5% of the water data within the  $\pm 30\%$  error band.

**Keywords:** Microchannel, Boiling number, Saturated critical heat flux (CHF), Length-to-diameter ratio, Weber number, Capillary number

#### 1. INTRODUCTION

Flow boiling in micro/mini-channels is encountered in energy and process systems including miniature heat exchangers, cooling of high-powered electric systems, catalytic reactors, miniature refrigeration systems, fuel injection systems of some internal combustion equipment, and evaporator components of fuel cells, among others [1]. However, one of the limiting operating conditions with flow boiling is the critical heat flux (CHF) or burnout, which refers to the replacement of

liquid being in contact with the heated surface with a vapor blanket. Thus, a wet-wall, high heat transfer coefficient operating condition transitions to a dry-wall, low heat transfer coefficient condition, resulting in the sudden increase of the heated surface temperature and possible failure of devices. The ability to predict CHF is therefore of vital importance for the safe operation.

CHF generally occurs at the channel outlet. According to whether the bulk fluid at the channel outlet is subcooled or not when CHF occurs, flow boiling CHF can be classified as either subcooled CHF or saturated CHF. In saturated CHF, the thermodynamic equilibrium vapor quality at the channel outlet is greater than or equal to zero but less than one, which is typically encountered at low mass velocities, at low inlet subcoolings and in channels with a relatively large length-to-diameter ratio.

Recently, for saturated flow boiling in micro/mini-channels, Warriar et al. [2] and Qu and Mudawar [3] observed that flow pattern developed into annular flow quickly. Sumith et al. [4] and Petterson [5] also presented a dominance of annular flow. In such flow patterns, most of the liquid flows in a thin liquid film along the wall and vapor flows mostly in the core of the channel. It is then reasonable to suggest that saturated CHF is most likely caused by the dry-out of the annular liquid film near the channel outlet. At low flow rates in micro/mini-channels, this type of CHF may be prone to occur due to the thinner liquid film thickness. Roday and Jensen [6, 7] studied the CHF condition of water and R123 during flow boiling in micro-tubes. The typical dry-out type behavior was seen in high-quality saturated region when the flow is completely annular. The annular flow patterns in the visualization study of Kosar and Peles [8] and Kosar et al. [9] also supported that dry-out is the mechanism of saturated CHF in micro/mini-channels.

A tricky aspect in micro/mini-scale studies is how to identify the macro-to-micro-scale threshold. That means, how small a channel could be called a micro/mini-channel that its behavior starts to deviate from the predictions of conventional macro-

channels. Mehendal et al. [10] proposed a classification based on fixed channel hydraulic diameters as follows: micro-channels (1-100  $\mu\text{m}$ ), meso-channels (100-1000  $\mu\text{m}$ ), macro-channels (1-6 mm) and conventional channels ( $>6$  mm). Kandlikar and Grande [11] also tried to identify the conventional-to-micro/mini-channel threshold by arbitrarily adopting an absolute diameter of 3 mm based on the characteristic tube diameter in distinct applications. It is important to highlight the fact that such criteria do not reflect the influence of channel size on physical mechanisms. Kew and Cornwell [12] proposed an approximate physical criterion for macro-to-micro-scale threshold diameter based on the growing bubble confinement as follows:

$$d_{th} = \left( \frac{4\sigma}{g(\rho_l - \rho_g)} \right)^{1/2} \quad (1)$$

According to this criterion, the macro-to-micro-scale transitional diameter may vary from a value as high as 5 mm for water at low reduced pressures to values smaller than 1 mm for  $\text{CO}_2$  at reduced pressures higher than 0.8. Although considering the surface-tension forces in this criterion, Kew and Cornwell [12] ignored the viscous forces, and did not present a careful comparison against thermal and dynamic behaviors for flow boiling in macro- and micro-channels. Recently, Li and Wu [13] analyzed an evaporative heat-transfer database and proposed a new transitional criterion by introducing the Bond number and the liquid Reynolds number, taking into account the differences in two-phase flow and heat transfer processes between micro/mini-channels and conventional channels. The combined non-dimensional number  $\text{BoRe}_l^{0.5} = 200$  was set as the conventional-to-micro/mini-channel criterion. When  $\text{BoRe}_l^{0.5} \leq 200$ , micro/mini-channel phenomenon dominates; when  $\text{BoRe}_l^{0.5} > 200$ , conventional macro-channel theory can explain the experimental data. Further, Li and Wu [14] collected a pressure-drop database and provided support for the  $\text{BoRe}_l^{0.5} = 200$  criterion.

We collected a large number of experimental data of different fluids for saturated flow in small channels to calculate saturated CHF for both multi- and single-channel configurations. Then, the database was analyzed by using various existing correlations to verify their respective accuracies. In addition, the  $\text{BoRe}_l^{0.5} = 200$  transitional criterion proposed by Li and Wu [13] was verified in saturated CHF analyses. Finally, generalized correlations were developed according to different length-to-diameter ratios, for various working fluids, channel sizes, and operating conditions.

## 2. REVIEW OF EXISTING DATA AND CORRELATIONS

### 2.1 Literature review

There are published papers [4, 6-8, 15-40] discussing saturated-flow boiling critical heat flux (CHF) in small

channels, covering the fluids R134a, R123, R236fa, R245fa, nitrogen, R12, and water at various mass fluxes, exit qualities and heat fluxes. There are two types of channel geometries: circular channels in highly conductive metal (copper, stainless steel) [4, 6, 7, 15, 16, 22, 24, 27-35, 37-40] and rectangular channels in silicon or metal substrate [8, 17-21, 23, 25, 26, 36, 37]. The latter can be heated non-uniformly. Tests were conducted for single-channel [4, 6, 7, 15, 16, 22, 24, 27-36] or multi-channel [8, 17-21, 23, 25, 26] configurations. For channels with hydraulic diameter larger than 3 mm, the flow in channels is vertical upward flow [28-30, 32-38]. In addition, boiling instabilities are a vital issue in flow boiling and can lead to premature CHF. Upstream compressible volume instability and excursive instability [41] are two major instabilities detected in micro/mini-channels. In single-channel arrangement, excursive instabilities can be cured by installing a throttle valve in the inlet line [6, 7, 16, 24, 27]; however, inlet orifices are needed to suppress the upstream compressible volume instability in multi-channel arrangements [8, 17, 18, 23, 26]. It is insufficient to install only a throttle valve before the header in multi-channel configurations [19-21, 25]; that will cure only one type of instability but not the other.

**Table 1. Descriptions of Four Empirical Existing Correlations.**

Author	Equation
Katto [45]	$Bl = 0.10 \left( \frac{\rho_v}{\rho_l} \right)^{0.133} \left( \frac{1}{We_{lo}} \right)^{0.333} \frac{1}{1 + 0.03L_h / d_h}$
Qu and Mudawar [25]	$Bl = 33.43 \left( \frac{\rho_v}{\rho_l} \right)^{1.11} We_{lo}^{-0.21} \left( \frac{L_h}{d_{he}} \right)^{-0.36}$
Wojtan et al. [24]	$Bl = 0.437 \left( \frac{\rho_v}{\rho_l} \right)^{0.073} We_{lo}^{-0.24} \left( \frac{L_h}{d_h} \right)^{-0.72}$
Qi et al. [27]	$Bl = (0.214 + 0.14Co) \left( \frac{\rho_v}{\rho_l} \right)^{0.133} \left( \frac{1}{We_{lo}} \right)^{0.333} \frac{1}{1 + 0.03L_h / d_h}$

Reliable prediction methods are needed in equipment design. Revellin and Thome [42] developed a model to predict CHF by solving the continuity, momentum and energy equations for an annular flow without interfacial waves. It is complicated because of the iterative procedure. Moreover, it was not wholly validated for rectangular micro-channels [43]. Kandlikar [44] also obtained a scale analysis based theoretical force balance model. The constants in the model were calculated from the available experimental data. Compared with the theoretical methods, empirical methods are simpler, but they are usually based only upon selected sets of experimental data or their own data. Table 1 lists several existing empirical

correlations. The Katto correlation [45] is a correlation for macro-channels. Qu and Mudawar [25] developed a correlation based on the saturated CHF results of water flowing in rectangular multi-microchannels. Wojtan et al. [24] investigated CHF characteristics of R134a and R245fa in tubes with 0.5 and 0.8 mm internal diameter, and proposed a saturated CHF prediction method by modifying the Katto-Ohno correlation.

## 2.2 Database description

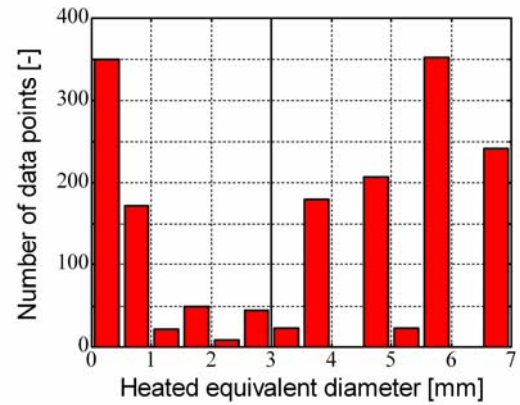
A saturated CHF database for small channels was obtained with 1,672 data points from 28 different datasets, covering 7 different working fluids. In the present work, the datasets which explicitly reported simultaneous values of exit quality, heat flux, mass flux, and saturation pressure were included. For the published datasets which reported length-to-diameter ratio or the heated length and not quality, only the ones presenting inlet sub-cooling values simultaneously were considered. Therefore, the information of the CHF can be recreated with certainty. In addition, some data points were not included because the data points immediately following them at nearly the same conditions had not yet achieved the CHF.

The distribution of the database against heated equivalent diameter ( $d_{he}$ ) is shown in Fig. 1a. Heated equivalent diameter ( $d_{he}$ ) covers a wide range of  $0.223 \leq d_{he} \leq 6.92$  mm. About 350 data points have heated equivalent diameters smaller than 0.5 mm, and 38.6% of the data points display a heated equivalent diameter smaller than 3 mm.

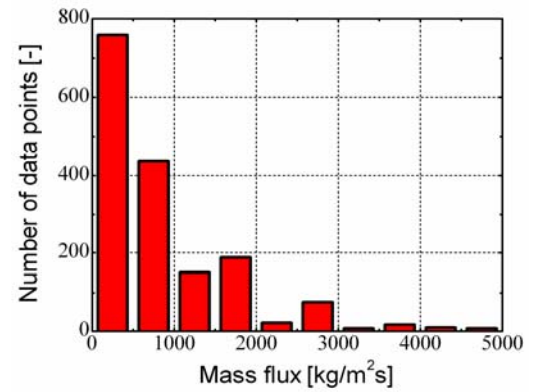
Figure 1b shows the repartition of the database against mass flux. The range of  $G$  is comprised between 23.4 and 5,200  $\text{kg/m}^2\text{s}$ . Almost 72% of the data points are in the region:  $G < 1,000$   $\text{kg/m}^2\text{s}$ , among which 63.5% are in the region:  $G < 500$   $\text{kg/m}^2\text{s}$ . Only 41 data points have mass fluxes larger than 3,000  $\text{kg/m}^2\text{s}$ .

Figure 2 presents the combined non-dimensional number  $\text{BoRe}_l^{0.5}$  versus the Bond number. The horizontal solid red line represents the macro-to-micro-scale transition developed by Li and Wu [13], which identifies the micro-scale region when  $\text{BoRe}_l^{0.5} \leq 200$ . Based on this criterion, about 51.4% of the entire database belongs to the micro/mini-scale region. Although the hydraulic diameter is as large as 6 mm, the combined non-dimensional number  $\text{BoRe}_l^{0.5}$  can be smaller than 200 for water, which is the fact in experiments of Kim et al. [33]. While the vertical dashed red line corresponds to the macro-to-micro-scale transition proposed by Kew and Cornwell [12], which defines the micro-scale region when  $d_h \leq d_{th}$ , yielding  $\text{Bo} \leq 4.0$ . According to this criterion, 48.0% of the overall data points are located in the micro/mini-channel region.

Among the entire database (1,672 data points), there are 462 non-aqueous data points, and 397 data points for water, with values of  $\text{BoRe}_l^{0.5} \leq 200$ , comprising the micro/mini-channel database.



(a)



(b)

Fig. 1. Distribution of the Database Against Different Parameters.

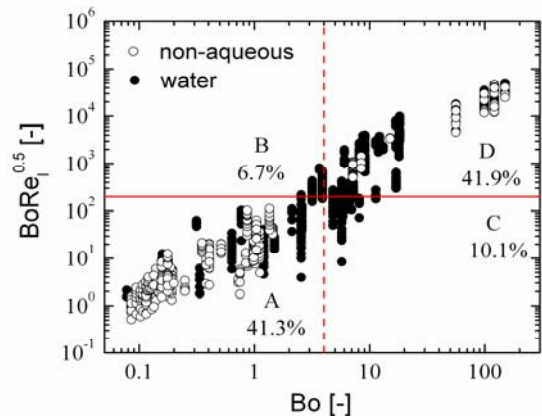


Fig. 2.  $\text{BoRe}_l^{0.5}$  vs.  $\text{Bo}$ .

### 2.3 Data comparison

The four saturated CHF correlations mentioned in Table 1 were evaluated by comparing them against the experimental database (only data points with  $BoRe_l^{0.5} \leq 200$  were included). It is of importance to say that properties of the fluids were taken at the outlet of the channel. Results of comparison of the data for non-aqueous fluids and water with existing prediction methods are depicted in Tables 2 and 3, respectively. The Wojtan et al. [24] correlation is the best among the three ones, predicting 69.3% of the micro/mini-channel database within the  $\pm 30\%$  error band. It performed well for its underlying data, Cavallini et al.'s data [15], Agostini et al.'s data [26], and Park and Thome's R134a data [23]. This correlation predicts Kosar and Peles's R123 data [8] with less accuracy, predicting 80.0% of the data points within the  $\pm 30\%$  error band. The Katto correlation [45] predicts 83.3% of Park and Thome's R245fa data [23] within the  $\pm 30\%$  error band. While the Qi et al. correlation [27] can only predict its underlying data, about 80.6% of the data within the  $\pm 30\%$  error band.

As shown in Table 3, neither the Wojtan et al. correlation [24] nor the Katto correlation [45] can obtain reasonable predictive values. The Qu and Mudawar correlation [25] performed accurately for its underlying data and Steinke and Kandlikar's data [16]. However, it can only predict 18.4% of the overall micro/mini-channel database within the  $\pm 30\%$  error band, so it can not be used as a predictive tool for a large database.

It is important to emphasize that deviations from the experimental trends are not necessarily related to weaknesses in the correlations themselves, but more to the unique nature of flow boiling in micro/mini-channels. New predictive tools must be developed to yield more accurate predictions.

### 3. RESULTS AND DISCUSSIONS

As mentioned above, data points with  $BoRe_l^{0.5} > 200$  were not adopted in the development of the new correlation because they are not located in the micro/mini-scale region. Heat flux is non-dimensional with mass flux and latent heat in boiling number  $Bl$ . Since  $Bl$  combines two important parameters,  $q$  and  $G$ , it is widely used in empirical treatment of flow boiling. Figure 3 shows that boiling number at CHF,  $Bl_{CHF}$ , has a strong relationship with length-to-diameter ratio  $L_h/d_{he}$ .

$$\begin{aligned} Bl_{CHF} &= q_{CHF} / (G \cdot h_{lv,e}) \\ h_{lv,e} &= h_{lv}(P_e) \end{aligned} \quad (2)$$

$q_{CHF}$  is the internal wall heat flux at CHF conditions.

As shown in Fig. 3, boiling number at CHF ( $Bl_{CHF}$ ) decreases greatly with length-to-diameter ratio  $L_h/d_{he}$  when  $L_h/d_{he}$  is small. This phenomenon can be explained from several aspects. First, Celata et al. [47] presented that the functional dependence

between the CHF and length-to-diameter ratio may be due to the incompletely thermal boundary layer for short channels. While Tong and Tang [48] discussed that the heated length effect comes from the entrance turbulence effect. In addition, in case of liquid film dryout CHF (saturated CHF) mechanism, heated length effects become more obvious and can exist up to longer tubes (Moon et al. [49]). Further, in experiments carried out by Nariai et al. [50] for short tubes, the smaller length-to-diameter ratio gave a larger CHF value with other system parameters being kept the same, and this effect becomes more significant for smaller channel diameters. That means the heated length effect is more noticeable in micro/mini-channels, different from that in conventional channels.

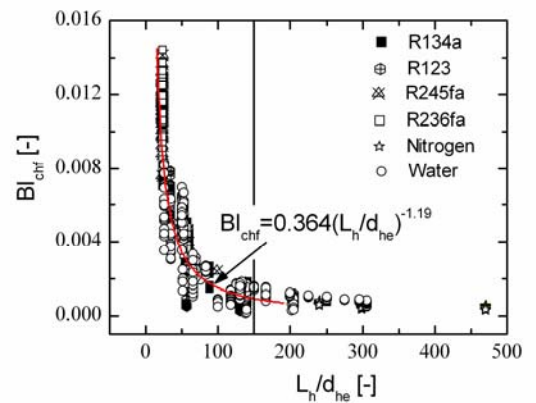


Fig. 3.  $Bl_{CHF}$  vs.  $L_h/d_{he}$  When  $BoRe_l^{0.5} \leq 200$ .

A relatively smooth trend occurs when  $L_h/d_{he} > 150$ . That means the length-to-diameter ratio presents negligible effect on boiling number when  $L_h/d_{he} > 150$ .

On one hand, for the region  $L_h/d_{he} \leq 150$ , a function can be obtained by regression method.

$$Bl_{CHF} = 0.364(L_h/d_{he})^{-1.19} \quad (3)$$

Function Y1 is defined as:

$$Y1 = Bl_{CHF} / (L_h/d_{he})^{-1.19} \quad (4)$$

The dependence of function Y1 on exit vapor quality  $x_e$  was presented in Fig. 4 for the entire database. From Eq. (5), the effects of inlet subcooling and outlet pressure on saturated CHF are partly attributed in exit quality.

$$x_e = \frac{1}{h_{lv,e}} \cdot \left( \frac{q_{CHF}}{G} - \overline{c_{pl}} \cdot \Delta T_{sub} \right) \quad (5)$$

$$\overline{c_{pl}} = c_{pl}(\overline{T}), \quad \overline{T} = (T_{sat}(P_e) + T_{in})/2$$

**Table 2. Experimental Non-aqueous Database Compared With the Prediction Methods When  $BoRe_1^{0.5} \leq 200$ .**

Authors	Fluid	No. of data points	Wojtan et al. [24]			Katto [45]			Qi et al. [27]			New correlation		
			$\lambda$	$e_A^*$	$\sigma_N^+$	$\lambda$	$e_A$	$\sigma_N$	$\lambda$	$e_A$	$\sigma_N$	$\lambda$	$e_A$	$\sigma_N$
Cavallini et al. [15]	R134a	7	<u>100.0</u>	12.7	2.5	0.0	54.3	1.1	0.0	51.0	3.8	<u>100.0</u>	14.8	3.0
Roday and Jensen [6-7]	R123	96	34.4	160.1	188.5	44.8	85.6	120.4	0.0	763.3	427.0	<u>87.5</u>	19.7	22.1
Kosar and Peles [8]	R123	30	80.0	18.6	19.0	53.3	27.1	17.3	0.0	374.7	112.8	<u>90.0</u>	12.0	14.6
Park and Thome [23]	R134a	76	96.0	10.9	13.3	32.9	35.1	11.4	0.0	187.7	36.1	<u>100.0</u>	11.4	8.87
-	R236fa	81	77.8	18.1	22.6	50.6	28.3	19.4	0.0	223.0	43.5	<u>100.0</u>	8.4	8.1
-	R245fa	84	53.6	26.9	20.6	83.3	20.3	23.8	0.0	306.4	88.1	<u>100.0</u>	8.7	6.9
Wojtan et al. [24]	R134a	29	93.2	13.2	14.2	0.0	38.6	3.6	0.0	162.2	21.6	<u>100.0</u>	7.1	3.6
-	R245fa	4	<u>100.0</u>	4.8	7.1	25.0	35.1	6.0	0.0	220.6	29.7	<u>100.0</u>	9.2	11.6
Agostini et al. [26]	R236fa	24	<u>100.0</u>	8.3	7.7	25.0	36.7	9.6	0.0	241.9	49.6	<u>100.0</u>	4.4	5.3
Qi et al. [27]	Nitrogen	31	64.5	23.7	18.0	0.0	70.1	7.5	<u>80.6</u>	22.8	18.1	80.6	20.5	22.3
		462	69.3	46.1	105.1	43.7	46.0	69.1	5.4	313.4	312.5	<b>95.5</b>	12.6	14.9

$$* e_R = \frac{1}{N_p} \cdot \sum_{i=1}^{N_p} \left[ \frac{(Bl_{CHF})_{cal} - (Bl_{CHF})_{exp}}{(Bl_{CHF})_{exp}} \right] \cdot 100, \quad e_A = \frac{1}{N_p} \cdot \sum_{i=1}^{N_p} \left| \frac{(Bl_{CHF})_{cal} - (Bl_{CHF})_{exp}}{(Bl_{CHF})_{exp}} \right| \cdot 100; \quad e_i = \left[ \frac{(Bl_{CHF})_{cal} - (Bl_{CHF})_{exp}}{(Bl_{CHF})_{exp}} \right] \cdot 100, \quad \sigma_N = \sqrt{\frac{\sum_{i=1}^{N_p} (e_i - e_R)^2}{N_p - 1}} \cdot 100$$

For the data points with  $BoRe_1^{0.5} \leq 200$ , function Y1 was strongly dependent on exit quality  $x_e$  from Fig. 4. When  $x_e$  increases, Y1 increases. A correlation was determined using least square fitting with experimental data.

$$Y1 = 0.62x_e^{0.82} \quad (6)$$

While for the ones with  $BoRe_1^{0.5} > 200$ , there is no apparent relationship between function Y1 and  $x_e$ . The difference demonstrates the macro-to-micro/mini-scale transitional criterion  $BoRe_1^{0.5} = 200$ .

Finally, for the region where  $L_h/d_{he} \leq 150$  and  $BoRe_1^{0.5} \leq 200$ , a new simple CHF correlation was developed.

$$Bl_{CHF} = q_{CHF} / (G \cdot h_{lv,e}) = 0.62 \cdot (L_h / d_{he})^{-1.19} \cdot x_e^{0.82} \quad (7)$$

On the other hand, for the region  $L_h/d_{he} > 150$  where heated length effects can be ignored, Fig. 5 presented the dependence of the boiling number on the combined non-dimensional number  $We_m Ca_1^{0.8}$  by considering the entire database. A log linear relationship between the boiling number Bl and  $We_m Ca_1^{0.8}$

was obtained for the data points with  $BoRe_1^{0.5} \leq 200$ . Thus, for the region where  $L_h/d_{he} > 150$  and  $BoRe_1^{0.5} \leq 200$ ,

$$Bl_{CHF} = 1.16 \times 10^{-3} (We_m Ca_1^{0.8})^{-0.16} \quad (8)$$

$$We_m = \frac{G^2 d_h}{\rho_m \sigma}, \quad \frac{1}{\rho_m} = \frac{x}{\rho_v} + \frac{1-x}{\rho_l}$$

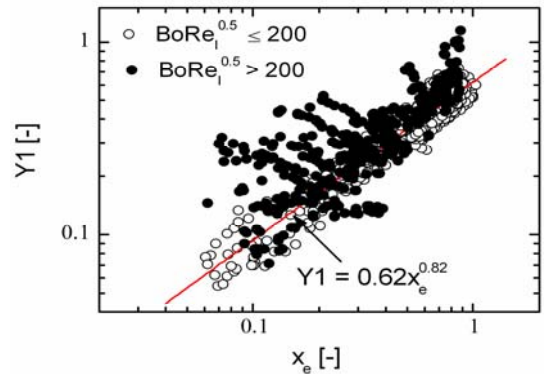


**Fig. 4. Y1 vs.  $x_e$  for  $L_h/d_{he} \leq 150$ .**

**Table 3. Experimental Database for Water Compared With the Prediction Methods When  $BoRe_1^{0.5} \leq 200$ .**

Author	No. of data points	Wojtan et al. [24]			Katto [45]			Qu and Mudawar [25]			New correlation		
		$\lambda$	$e_A^*$	$\sigma_N^+$	$\lambda$	$e_A$	$\sigma_N$	$\lambda$	$e_A$	$\sigma_N$	$\lambda$	$e_A$	$\sigma_N$
Roday et al. [16]	15	0.0	419.0	122.8	0.0	181.7	66.7	13.3	66.5	69.3	<u>80.0</u>	21.5	18.3
Roday and Jensen [6-7]	27	0.0	193.5	197.9	33.3	75.8	117.5	33.3	44.4	49.7	<u>92.6</u>	14.7	16.9
Kosar et al. [17]	4	0.0	250.9	70.2	0.0	130.5	57.2	0.0	68.3	21.0	<u>100.0</u>	10.2	9.3
Kuo and Peles [18]	25	0.0	235.9	61.8	0.0	161.6	66.0	0.0	76.6	15.9	<u>100.0</u>	15.4	6.2
Sumith et al. [4]	6	0.0	192.4	75.7	0.0	153.4	100.0	16.7	48.8	11.1	<u>100.0</u>	13.0	3.0
Kuan and Kandlikar [19-20]	6	0.0	185.0	28.0	0.0	122.9	46.0	16.7	35.1	4.4	<u>100.0</u>	18.3	1.2
Steinke and Kandlikar [21]	5	0.0	295.9	46.6	0.0	126.2	19.9	<u>100.0</u>	13.3	17.1	60.0	23.3	28.8
Yu et al. [22]	27	7.4	108.3	73.3	51.9	44.0	52.9	51.9	39.0	44.2	<u>92.6</u>	27.0	2.6
Qu and Mudawar [25]	18	0.0	295.5	17.4	0.0	188.0	24.7	<u>100.0</u>	5.1	6.0	<u>100.0</u>	11.1	7.3
Kim et al. [33]	84	0.0	332.2	48.8	0.0	316.1	55.3	22.6	208.9	191.4	<u>89.3</u>	15.7	13.8
Kureta et al. [34]	56	0.0	373.3	142.4	10.7	217.3	230.1	3.6	61.6	19.2	<u>100.0</u>	9.8	8.9
Kureta et al. [35]	8	0.0	314.0	110.3	0.0	133.6	45.0	0.0	62.8	11.1	<u>87.5</u>	20.2	10.3
Mishima et al. [36]	43	0.0	1090	319.2	0.0	1432	677.3	4.7	112.8	63.0	<u>100.0</u>	9.4	6.2
De Bortoli et al. [37]	49	0.0	243.4	102.2	0.0	324.0	159.6	0.0	2759	1804	<u>93.9</u>	15.0	14.2
Becker et al. [38]	11	0.0	156.8	40.8	0.0	57.1	17.5	0.0	1509	508.0	<u>63.6</u>	30.3	27.6
Firstenberg et al. [39]	5	0.0	165.9	76.1	0.0	188.2	124.2	0.0	631.5	176.4	<u>100.0</u>	20.1	1.1
Weatherhead [40]	8	0.0	194.9	56.2	0.0	90.9	33.7	0.0	1465	306.2	<u>100.0</u>	9.3	12.8
	397	0.5	365.6	281.2	7.3	321.2	438.7	18.4	431.6	1051	<b>93.5</b>	18.6	19.1

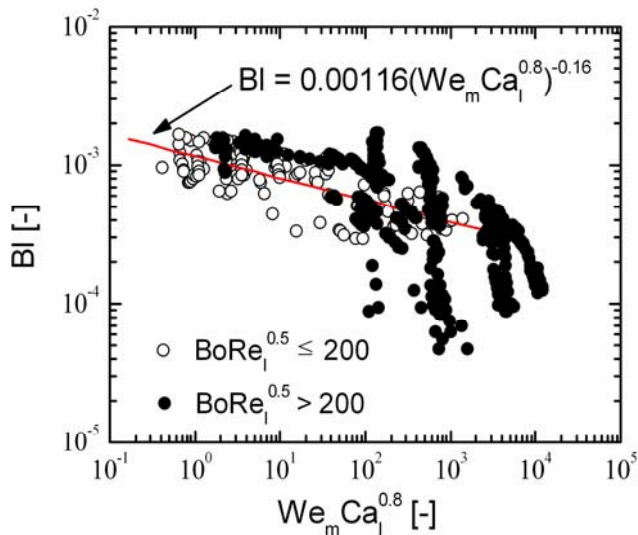


**Fig. 5. BI vs.  $We_m Ca_l^{0.8}$  for  $L_h/d_{he} > 150$ .**

**Table 4. Evaluation of the Two Proposed Correlations When  $BoRe_1^{0.5} \leq 200$ .**

Correlatio n	Number of data points	$e_R$	$e_A$	$\sigma_N$	$\lambda$
(a) $L_h/d_{he} \leq 150$					
Eq. (7)	726	2.3	10.2	13.7	96.8
(b) $L_h/d_{he} > 150$					
Eq. (8)	133	-5.9	16.1	20.5	82.0

Equation (7) is a general micro/mini-channel correlation applied for channels with  $L_h/d_{he} \leq 150$ , while Eq. (8) is the one used for relatively long channels with  $L_h/d_{he} > 150$ . When evaluating the newly developed correlations against the collected micro/mini-channel database, Eq. (7) and Eq. (8) were adopted for  $L_h/d_{he} \leq 150$  and  $L_h/d_{he} > 150$ , respectively. The underlined figures are the largest among the percentages of data within the  $\pm 30\%$  error band predicted by the four existing correlations for saturated CHF. It is obvious that the new method is the best one, which predicts almost 95.5% of the non-aqueous data points and 93.5% of the water data within the  $\pm 30\%$  error band. It performs well for the micro/mini-channel database. It can accurately predict saturated CHF in micro-channels with refrigerants, water, or nitrogen. It is important to notify that all fluid properties should be taken at the outlet of the channel.

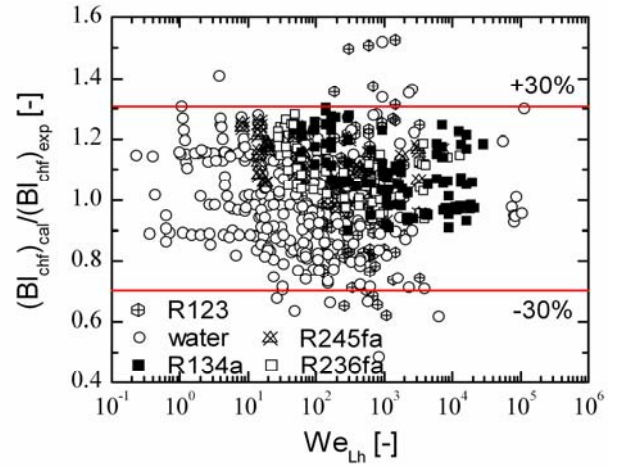
As shown in Table 4, 726 data points were predicted by Eq. (7), about 96.8% of them were located in the  $\pm 30\%$  error band, and 133 data points were evaluated by Eq. (8), 82.0% of them were located in  $\pm 30\%$  error band.

Figures 6a and 6b compare Eq. (7) and Eq. (8) with the micro/mini-channel database of different Weber number  $We_{Lh}$  for  $L_h/d_{he} \leq 150$  and  $L_h/d_{he} > 150$ , respectively. The heated length was used in the calculation of  $We_{Lh}$ .

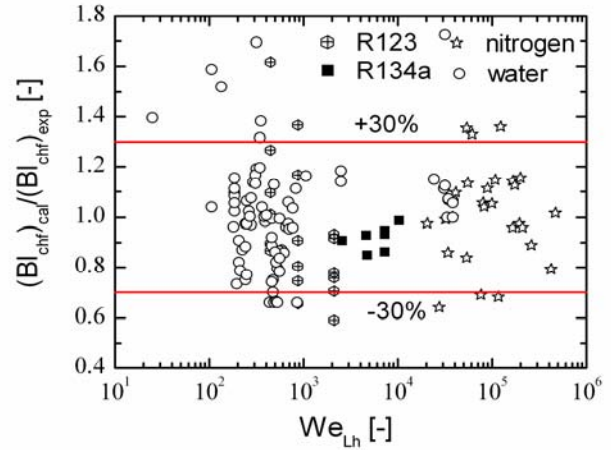
$$We_{Lh} = G^2 L_h / (\rho_l \sigma) \quad (9)$$

All fluid properties are also taken at the outlet of the channel. Almost all values of the ratio of the predicted boiling number  $(Bl_{CHF})_{cal}$  by the new method to the experimental boiling number  $(Bl_{CHF})_{exp}$  are within the region from 0.7 to 1.3. In addition, there is no obvious relationship between the  $Bl_{CHF}$  ratio and the Weber number  $We_{Lh}$ . In conclusion, the new method is able to predict different working fluids flowing in various micro/mini-channels with dissimilar hydraulic diameters under different operational conditions.

Figure 7 shows the comparison between four existing correlations and the newly proposed correlations against four experimental datasets with heated equivalent diameters of 0.383, 1.042, 2.75, and 4.58 mm for three different fluids: R236fa, nitrogen, and water, respectively. The datasets in Figs. 7a, 7c, and 7d all have length-to-diameter ratios smaller than 150, while the length-to-diameter ratio in Fig. 7c is larger than 150. The Katto correlation [45] under-predicted Agostini et al.'s R236fa data [26], and it largely overrates Mishima et al.'s [36] and De Bortoli et al.'s [37] water data. The Qu and Mudawar correlation [25] also over-predicts Mishima et al.'s [36] and De Bortoli et al.'s [37] water data greatly. However, the new method can predict the datasets well on the whole, and is more consistent than the other four correlations.

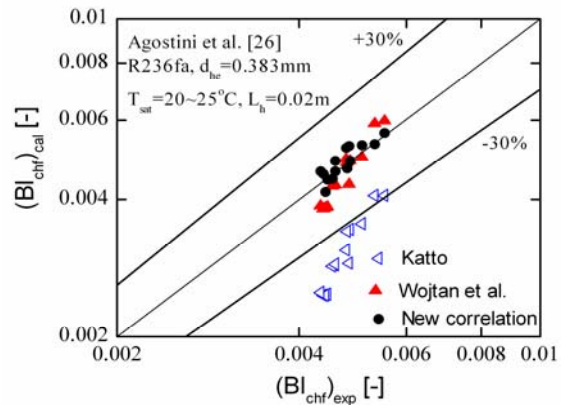


(a)  $L_h/d_{he} \leq 150$

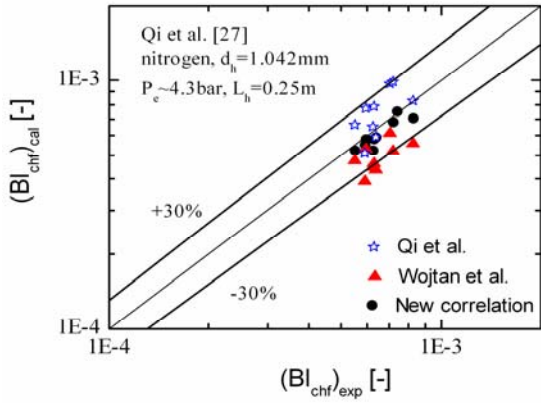


(b)  $L_h/d_{he} > 150$

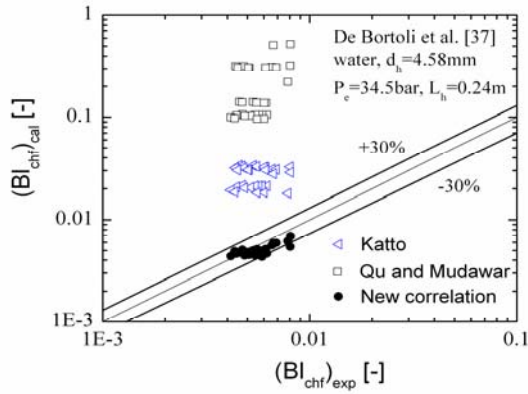
**Fig. 6. Comparison of the New Method With the Micro/mini-channel Database of Different Weber Number  $We_{Lh}$  When  $BoRe_l^{0.5} \leq 200$ .**



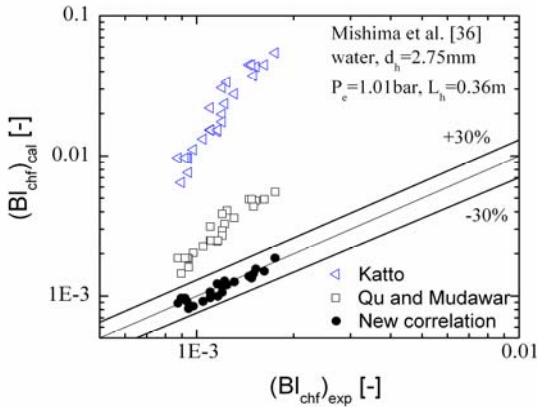
(a)



(b)



(c)



(d)

**Fig. 7. Verification of the Newly Proposed Method Against Experimental Datasets. (The four empirical existing correlations are shown as a reference of comparison).**

#### 4. CONCLUSIONS

- 1) A database (1,672 data points) of saturated critical heat flux (CHF) in micro/mini-channels from a variety of sources were compiled and analyzed. Among it 859 data

points with  $BoRe_1^{0.5} \leq 200$  were compared with four empirical correlations. The Wojtan et al. correlation [24] can predict 69.3% of the non-aqueous data within the  $\pm 30\%$  error band. The Qu and Mudawar correlation [25] performed accurately only for its underlying water data and Steinke and Kandlikar's water data [21]. The Katto correlation [45] presented drastically different results for different datasets.

- 2) The boiling number at CHF,  $BI_{CHF}$ , decreases greatly with length-to-diameter ratio  $L_h/d_{he}$  when  $L_h/d_{he}$  is small. While the length-to-diameter ratio presents negligible effect on boiling number when  $L_h/d_{he} > 150$ . For the region where  $L_h/d_{he} \leq 150$  and  $BoRe_1^{0.5} \leq 200$ , a simple saturated CHF correlation was proposed by using the boiling number, length-to-diameter ratio, and exit quality. A combined dimensionless number  $We_m Ca_1^{0.8}$  was introduced to correlate the micro/mini-channel database for the region where  $L_h/d_{he} > 150$ . It should be noted that all properties should be taken at outlet of the channel. The new method can predict the overall micro/mini-channel database accurately on the whole. It can predict almost 95.5% of the non-aqueous data and 93.5% of the water data within the  $\pm 30\%$  error band.
- 3) Considering the entire database, data points where  $BoRe_1^{0.5} \leq 200$  and  $BoRe_1^{0.5} > 200$  show very different trends, as shown in Figs .5 and 6, which provide strong support to the macro-to-micro/mini-scale criterion proposed by Li and Wu [13].

#### NOMENCLATURE

BI	boiling number, $q/(Gh_{lv})$ (-)
Bo	Bond number, $g(\rho_l - \rho_g)d_h^2/\sigma$ (-)
Ca <sub>l</sub>	Capillary number, $\mu_l G/(\rho_l \sigma)$ (-)
$c_{pl}$	constant-pressure specific heat of liquid (J/kg·K)
$d_h$	channel hydraulic diameter (m)
$d_{he}$	heated equivalent diameter (m)
$d_{th}$	macro-to-micro-scale threshold diameter proposed by Kew and Cornwell [12] (m)
$e_A$	mean absolute error (%)
G	mass flux ( $kg/m^2 \cdot s$ )
g	gravitational acceleration ( $m/s^2$ )
$h_{lv}$	latent heat of vaporization (J/kg)
$L_h$	heated length (m)
P	pressure (Pa)
q	heat flux ( $kW/m^2$ )
$Re_1$	liquid Reynolds number, $G(1-x)d_h/\mu_l$ (-)
We	Weber number, $G^2 d_h/(\rho \sigma)$ (-)
x	thermodynamic vapor quality, (-)
Y1	parameter used in Equation (4)

#### Greek symbols

$\lambda$	percentage of data within $\pm 30\%$ error band (%)
$\mu$	dynamic viscosity (Pa·s)
$\rho$	density ( $kg/m^3$ )

$\sigma$	surface tension (N/m)
$\sigma_N$	standard deviation (%)
$\Delta T_{\text{sub}}$	inlet subcooling temperature (K)

#### Subscripts

cal	calculated
chf	critical heat flux
e	exit
exp	experimental
in	inlet
l	saturated liquid
lo	liquid only
m	average
sat	saturated
v	saturated vapor

#### ACKNOWLEDGMENTS

This study is funded by the National Natural Science Foundation (50976096), National High Technology Research and Development (863 Programme) (#2007AA05Z226), and Technology Research Program (2008R10026) of Zhejiang Province of China.

#### REFERENCES

- [1] I. Mudawar, Assessment of high-heat-flux thermal management schemes, in: IEEE Transactions on Component and Packaging Technologies 24 (2001) 122-141.
- [2] G.R. Warriar, V.K. Dhir, L.A. Momoda, Heat transfer and pressure drop in narrow rectangular channels, Experimental Thermal Fluid Science 26 (2002) 53-64.
- [3] W. Qu, I. Mudawar, Flow boiling heat transfer in two-phase micro-channel heat sinks--I. Experimental investigation and assessment of correlation methods, International Journal of Heat and Mass Transfer 46 (2003) 2755-2771.
- [4] B. Sumith, F. Kaminaga, K. Matsumura, Saturated flow boiling of water in a vertical small diameter tube, Experimental Thermal and Fluid Science 27 (2003) 789-801.
- [5] J. Pettersen, Flow vaporization of CO<sub>2</sub> in microchannel tubes, Experimental Thermal and Fluid Science 28(2004) 111-121.
- [6] A.P. Roday, M.K. Jensen, Experimental investigation of the CHF condition during flow boiling of water in microtubes, in: 2007 ASME-JSME Thermal Engineering Summer Heat Transfer Conference, July 8-12, Vancouver, Canada.
- [7] A.P. Roday, M.K. Jensen, Study of critical heat flux condition with water and R-123 during flow boiling in microtubes. Part I : Experimental results and discussion of parametric effects, International Journal of Heat and Mass Transfer 52 (2009) 3235-3249
- [8] A. Kosar, Y. Peles, Critical heat flux of R-123 in silicon-based microchannels, Journal of Heat Transfer 129 (2007) 844-851
- [9] A. Kosar, C.J. Kuo, Y. Peles, Suppression of boiling flow oscillations in parallel microchannels with inlet restrictors, Journal of Heat Transfer 128 (2006) 251-260.
- [10] S.S. Mehendal, A.M. Jacobi, R.K. Shah, Fluid flow and heat transfer at micro- and meso-scales with application to heat exchanger design, Applied Mechanics Reviews 53 (2000) 175-193.
- [11] S.G. Kandlikar, W.J. Grande, Evolution of micro-channel flow passages- Thermohydraulic Performance and Fabrication Technology, Heat Transfer Engineering, 25 (2002) 3-17.
- [12] P.A. Kew, K. Cornwell, Correlations for the prediction of boiling heat transfer in small-diameter channels, Applied Thermal Engineering 17 (1997) 705-715.
- [13] W. Li, Z. Wu, A general criterion for evaporative heat transfer in micro/mini-channels, International Journal of Heat and Mass Transfer 53 (2010) 1967-1976.
- [14] W. Li, Z. Wu, A general correlation for adiabatic two-phase pressure drop in micro/mini-channels, International Journal of Heat and Mass Transfer 53 (2010) 2732-2739.
- [15] A. Cavallini, S. Bortolin, and D.D. Col et al., Experiments on dry-out during flow boiling in a round minichannel, Bremen Microgravity Science Technology 2007 XIX-3/4.
- [16] A.P. Roday, T.B. Tasciuc, M.K. Jensen, The critical heat flux condition with water in a uniformly heated microtube, Journal of heat transfer 130 (2008) 1-9.
- [17] A. Kosar, C.J. Kuo, Y. Peles, Reduced pressure boiling heat transfer in rectangular microchannels with interconnected reentrant cavities, Journal of Heat Transfer 127 (2005) 1106-1114.
- [18] C.J. Kuo, Y. Peles, Critical heat flux of water at subatmospheric pressures in microchannels, Journal of Heat Transfer 130 (2008) 1-7.
- [19] W.K. Kuan, S.G. Kandlikar, Experimental study and model on critical heat flux of refrigerants-123 and water in microchannels, Journal of Heat Transfer 130 (2008) 034503, 1-5.
- [20] W.K. Kuan, S.G. Kandlikar, Experimental study on saturated flow boiling critical heat flux in microchannels, in: Fourth International Conference on Nanochannels, Microchannels and Minichannels, June 19-21, 2006, Limerick, Ireland.
- [21] M.E. Steinke, S.G. Kandlikar, An experimental investigation of flow boiling characteristics of water in parallel microchannels, Journal of Heat Transfer 126 (2004) 518-526.
- [22] W. Yu, D.M. France, and M.W. Wambsganss et al., Two-phase pressure drop, boiling heat transfer, and critical heat flux to water in a small-diameter horizontal tube, International Journal of Multiphase Flow 28 (2002) 927-941.
- [23] J. Park, J.R. Thome, Critical heat flux in multi-microchannel copper elements with low pressure refrigerants, International Journal of Heat and Mass Transfer 53 (2010) 110-122.

- [24] L. Wojtan, R. Revellin, J.R. Thome, Investigation of saturated critical heat flux in a single, uniformly heated microchannel, *Experimental Thermal and Fluid Science* 30 (2006) 765-774.
- [25] W. Qu, I. Mudawar, Measurement and correlation of critical heat flux in two-phase micro-channel heat sinks, *International Journal of Heat and Mass Transfer* 47 (2004) 2045-2059.
- [26] B. Agostini, R. Revellin, and J.R. Thome et al., High heat flux flow boiling in silicon multi-microchannels – Part III: Saturated critical heat flux of R236fa and two-phase pressure drops, *International Journal of Heat and Mass Transfer* 51 (2008) 5426-5442.
- [27] S.L. Qi, P. Zhang, and R.Z. Wang et al., Flow boiling of liquid nitrogen in micro-tubes: Part II – Heat transfer characteristics and critical heat flux, *International Journal of Heat and Mass Transfer* 50 (2007) 5017-5030.
- [28] X. Cheng, F.J. Erbacher, and U. Muller et al., Critical heat flux in uniformly heated vertical tubes, *International Journal of Heat and Mass Transfer* 40 (1997) 2929-2939.
- [29] I.L. Pioro, D.C. Groeneveld, L.K.H. Leung, S.S. Doerffer, S.C. Cheng, Yu.V. Antoshko, Y. Guo, A.Z. Vasic, Comparison of CHF measurements in horizontal and vertical tubes cooled with R-134a, *International Journal of Heat and Mass Transfer* 45 (2002) 4435-4450.
- [30] I.L. Pioro, S.C. Cheng, D.C. Groeneveld, A.Z. Vasic, S. Pinchon, G. Chen, Experimental study of the effect of non-circular flow geometry on the critical heat flux, *Nuclear Engineering and Design* 187 (1999) 339-362.
- [31] R. Yun, Y.C. Kim, Critical quality prediction for saturated flow boiling of CO<sub>2</sub> in horizontal small diameter tubes, *International Journal of Heat and Mass Transfer* 46 (2003) 2527-2535.
- [32] A. Olekhovitch, A. Teyssedou, P. Tye, Critical heat flux in a vertical tube at low and medium pressures. Part II - new data representation, *Nuclear Engineering and Design* 193 (1999) 91-103.
- [33] H.C. Kim, W.P. Baek, S.H. Chang, Critical heat flux of water in vertical round tubes at low pressure and low flow conditions, *Nuclear Engineering and Design* 199 (2000) 49-73.
- [34] M. Kureta, K. Mishima, H. Nishihara, Critical heat flux for flow-boiling of water in small-diameter tubes under low-pressure conditions, in: *Proceedings of JSME* 61 (1995) 311-318.
- [35] M. Kureta, K. Mishima, H. Nishihara, K. Tasaka, Effects of diameter and heated length on critical heat flux for water flowing in small-diameter tubes, in: *Proceedings of JSME* 60 (1995) 217-222.
- [36] K. Mishima, T. Hibiki, H. Nishihara, T. Motomura, T. Otsuji, A. Kurosawa, Experimental study on critical heat flux in laterally non-uniformly heated rectangular channels, Yuge National College of Maritime Technology, NII-Electronic Library Service.
- [37] R. A. De Bortoei, S. J. Green et al., Forced convection heat transfer burnout studies for water in rectangular channels and round tubes at pressure above 500 psia, WAPD-188 (1958).
- [38] K.M. Becker, Measurements of burnout conditions for flow of boiling water in vertical round ducts (part 2), A.E. 114 (1963).
- [39] H. Firstenberg, K. Goldmann, L.L. Bianco, S. Preiser, G. Rabinowitz, Compilation of experimental forced convection quality burnout data with calculated Reynolds numbers, N.D.A. 2131 (1960).
- [40] R.J. Weatherhead, Heat transfer flow instability and critical heat flux for water in a small tube at 200 psia, A.N.L. 6715(1963).
- [41] A.E. Bergles, S.G. Kandlikar, On the nature of critical heat flux in microchannels, *Journal of Heat Transfer* 127 (2005) 101-107.
- [42] R. Revellin, J.R. Thome, A theoretical model for the prediction of the critical heat flux in heated microchannels, *International Journal of Heat and Mass Transfer* 51 (2008) 1216-1225.
- [43] A. Kosar, A model to predict saturated critical heat flux in minichannels and microchannels, *International Journal of Thermal Sciences* 48 (2009) 261-270.
- [44] S.G. Kandlikar, A scale analysis based theoretical force balance model for critical heat flux (CHF) during saturated flow boiling in microchannels and minichannels, in: *Proceedings of ASME 2009 2<sup>nd</sup> Micro/Nanoscale Heat & Mass Transfer International Conference*, Dec. 19-21, 2009, Shanghai, China.
- [45] Y. Katto, A generalized correlation of critical heat flux for the forced convection boiling in vertical uniformly heated round tubes, *International Journal of Heat and Mass Transfer* 21 (1978) 1527-1542.
- [46] J. Park, Critical heat flux in multi-microchannel copper elements with low pressure refrigerants, Ph.D. thesis, Swiss Federal Institute of Technology in Lausanne (EPFL), 2008, available at: <http://library.epfl.ch/theses/?nr=4223>.
- [47] G.P. Celata, M. Cumo, A. Mariani, M. Simoncini, G. Zummo, Rationalization of existing mechanistic models for the prediction of water subcooled flow boiling critical heat flux. *International Journal of Heat and Mass Transfer* 37 (1994) 347-360.
- [48] L.S. Tong, Y.S. Tang, *Boiling heat transfer and two phase flow*, Second edition, Taylor and Francis, USA, 1997.
- [49] S.K. Moon, W.P. Baek, S.H. Chang, Parametric trends analysis of the critical heat flux based on artificial neural networks, *Nuclear Engineering Design* 163 (1996) 29-49.
- [50] H. Nariyai, H. Kinoshita, T. Yoshida, F. Inasaka, Effect of tube length on the CHF of subcooled flow boiling, *Second Symposium on Multi-Phase Flow*, Tokyo, 1997, 211-221.